

# Cooling a nanomechanical resonator with quantum back-action

A. Naik<sup>1,2</sup>, O. Buu<sup>1,3</sup>, M. D. LaHaye<sup>1,3</sup>, A. D. Armour<sup>4</sup>, A. A. Clerk<sup>5</sup>, M. P. Blencowe<sup>6</sup> & K. C. Schwab<sup>1</sup>

Quantum mechanics demands that the act of measurement must affect the measured object. When a linear amplifier is used to continuously monitor the position of an object, the Heisenberg uncertainty relationship requires that the object be driven by force impulses, called back-action<sup>1–3</sup>. Here we measure the back-action of a superconducting single-electron transistor (SSET) on a radio-frequency nanomechanical resonator. The conductance of the SSET, which is capacitively coupled to the resonator, provides a sensitive probe of the latter's position; back-action effects manifest themselves as an effective thermal bath, the properties of which depend sensitively on SSET bias conditions. Surprisingly, when the SSET is biased near a transport resonance, we observe cooling of the nanomechanical mode from 550 mK to 300 mK—an effect that is analogous to laser cooling in atomic physics. Our measurements have implications for nanomechanical readout of quantum information devices and the limits of ultrasensitive force microscopy (such as single-nuclear-spin magnetic resonance force microscopy). Furthermore, we anticipate the use of these back-action effects to prepare ultracold and quantum states of mechanical structures, which would not be accessible with existing technology.

Back-action impulses arise in practice from the quantized and stochastic nature of the fundamental particles used in the measuring device. For example, in high precision optical interferometers such as the LIGO gravitational wave detector<sup>4</sup> or in the single-spin force microscope<sup>3</sup>, the position of a test mass is monitored by reflecting laser light off the measured object and interfering this light with a reference beam at a detector. The measured signal is the arrival rate of photons, and one might say that the optical 'conductance' of the interferometer is modulated by the position of the measured object. Back-action forces that stochastically drive the measured object result from the random impact and momentum transfer of the discrete photons. This mechanical effect of light is thought to provide the ultimate limit to the position and force sensitivity of an optical interferometer. Although this photon 'ponderomotive' noise has not yet been detected during the measurement of a macroscopic object<sup>6</sup>, these back-action effects are clearly observed and carefully used in the cooling of dilute atomic vapours to nanokelvin temperatures.

In the experiments reported here, we study an SSET that is capacitively coupled to a voltage-biased ( $V_{NR}$ ), doubly clamped nanomechanical resonator (Fig. 1). Like the interferometer, the conductance of the SSET is a very sensitive probe of the resonator's position, whereas the particles transported in this case are a mixture of single and Cooper-paired electrons. We have recently shown the SSET to be nearly a quantum-limited position detector<sup>7</sup>; however, reaching the best sensitivity will ultimately be limited by the back-action of the charged particles<sup>3</sup>, which could not be observed in previous experiments because of insufficient SSET–resonator coupling.

The back-action force of the SSET results in three measurable effects on the resonator: a frequency shift, a damping rate, and position fluctuations. The frequency shift and damping rate are caused by the in-phase and small out-of phase response in the average electrostatic force between the SSET and resonator, as the resonator oscillates. Position fluctuations arise from fluctuations in this force. As electrons and Cooper pairs are transported through the SSET island, the island charge changes stochastically by  $\pm 1$  or 2 electrons, causing the electrostatic force to fluctuate with an amplitude of  $10^{-13}N_{RMS}$ , with a white spectral density of  $S_F^{1/2} \approx 10^{-18}N\text{Hz}^{-1/2}$ , extending to  $\sim 20$  GHz (assuming  $V_{NR} = 2$  V and parameters given in Supplementary Information).

These back-action effects are observed by measuring the SSET charge noise in the vicinity of the resonator frequency (Supplementary Information), thus obtaining the resonator noise temperature,

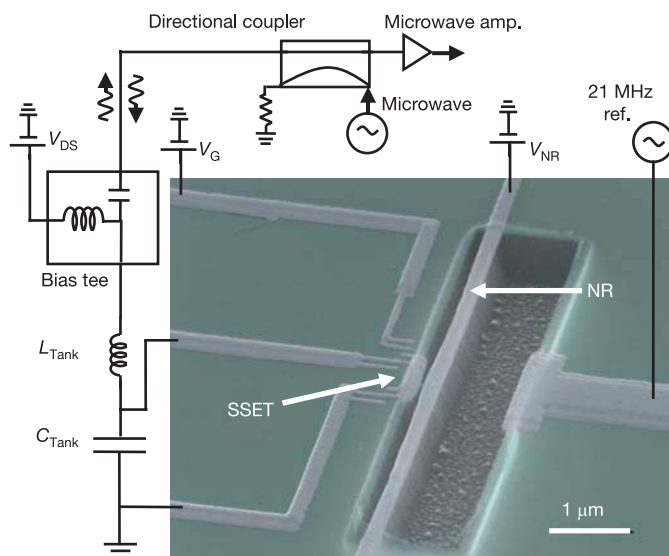


**Figure 1 | Nanodevice and measurement diagram.** Scanning electron microscope image of the device (false colour): a 21.9-MHz, doubly clamped, SiN and Al nanomechanical resonator (NR) coupled to a superconducting single-electron transistor (SSET), with simplified measurement circuit diagram. See Supplementary Information for sample parameters.  $V_G$ , gate voltage;  $V_{NR}$ , nanoresonator bias voltage;  $V_{DS}$ , drain–source voltage, applied through the bias tee. The SSET is read out by applying 1.17 GHz microwaves through the directional coupler, and monitoring the signal reflected off the LCR tank circuit formed by  $L_{Tank}$ ,  $C_{Tank}$  and the SSET. The charge sensitivity of the system is calibrated by a fixed 21 MHz reference voltage signal applied to a nearby gate capacitor.

<sup>1</sup>Laboratory for Physical Sciences, <sup>2</sup>Department of Electrical and Computer Engineering, <sup>3</sup>Department of Physics, University of Maryland, College Park, Maryland 20740, USA.

<sup>4</sup>School of Physics and Astronomy, University of Nottingham, Nottingham NG7 2RD, UK. <sup>5</sup>Department of Physics, McGill University, Montreal, QC Canada H3A 2T8.

<sup>6</sup>Department of Physics and Astronomy, Dartmouth College, Hanover, New Hampshire 03755, USA.

$T_{\text{NR}}$ , and dissipation rate,  $\gamma_{\text{NR}} = \omega_{\text{NR}}/Q_{\text{NR}}$ , for different coupling voltages,  $V_{\text{NR}}$ , and refrigerator temperatures,  $T_{\text{Bath}}$ ; here  $\omega_{\text{NR}}$  and  $Q_{\text{NR}}$  are the resonator angular frequency and quality factor. Figure 2 inset shows an example of the measured spectral noise power where the mechanical resonance at  $\omega_{\text{NR}} = 2\pi 21.837$  MHz is clearly visible, and accurately fits a simple harmonic oscillator response function, on top of a white power spectrum due to an ultralow-noise microwave preamplifier used to read out the SSET with microwave reflectometry<sup>8</sup>.

For low SSET–nanoresonator coupling strengths, and with the SSET biased close to the Josephson quasiparticle peak<sup>9</sup> (JQP),  $T_{\text{NR}}$  simply follows  $T_{\text{Bath}}$ , with the lowest temperature point corresponding to occupation number  $N_{\text{TH}} \approx 25$ , and the nanoresonator shows a very low dissipation rate ( $Q_{\text{NR}} = 120,000$  at  $T_{\text{Bath}} = 100$  mK); see Fig. 2. This is an elementary demonstration of the equipartition theorem and of nanomechanical noise thermometry<sup>7</sup>.

As the SSET bias point is held fixed at a JQP and the coupling voltage is increased, we find clear signatures of all three expected back-action effects. Figure 3 shows the change in resonance frequency and dissipation rate,  $\gamma_{\text{NR}}$ , caused by coupling to the SSET. The back-action fluctuation effects on  $T_{\text{NR}}$  first become noticeable for  $T_{\text{Bath}} < 200$  mK (Fig. 2), where we observe an increase and ultimately a saturation of  $T_{\text{NR}} \approx 200$  mK; the SSET back-action exerts a stochastic force drive, in excess of the thermal noise of  $T_{\text{Bath}}$ .

At our highest coupling strength,  $V_{\text{NR}} = 15$  V, we find that  $T_{\text{NR}}$  has a much weaker dependence on  $T_{\text{Bath}}$ , tending towards a fixed value of  $\sim 200$  mK. In this high coupling limit and for  $T_{\text{Bath}} > 200$  mK, we observe the counter-intuitive effect that a noisy, non-equilibrium measuring device can cool the nanomechanical mode.

This behaviour can be understood through models based on a quantum noise approach<sup>10</sup> or a master equation description of the coupled electro-mechanical system<sup>11</sup>. These models show that the back-action effects are that of an effective thermal bath; similar results have been obtained for oscillators coupled to other non-equilibrium devices: a normal state single-electron transistor<sup>12,13</sup>, a quantum point contact<sup>14</sup>, and in experiments with a ping-pong ball in turbulent air flow<sup>15</sup>. The resulting damping and temperature of the

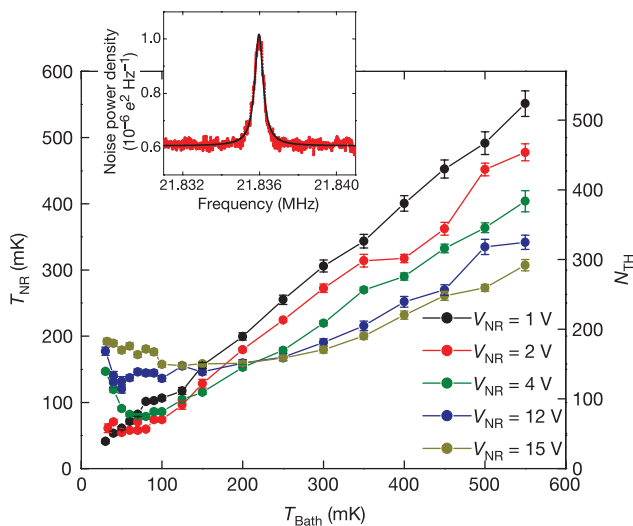


**Figure 2 | Resonator temperature versus bath temperature and coupling voltage.** Main plot shows the effective temperature of the resonator (in mK and quanta  $N_{\text{TH}}$ ),  $T_{\text{NR}}$ , versus bath temperature,  $T_{\text{Bath}}$ , with the SSET biased near the JQP. See text for discussion. Inset shows an example of the measured charge noise power (red trace), taken at  $T_{\text{Bath}} = 100$  mK and  $V_{\text{NR}} = 4$  V, and a Lorentzian fit (black line). The area of this peak is proportional to the resonator temperature,  $T_{\text{NR}}$ . Error bars are the standard deviation of the estimate of the total NR noise power.

resonator due to coupling to both refrigerator thermal bath ( $T_{\text{Bath}}$ ) and SSET effective bath ( $T_{\text{SSET}}$ ) through the associated damping rates ( $\gamma_{\text{Bath}}$  and  $\gamma_{\text{SSET}}$ ) are then given by:

$$\gamma_{\text{NR}} = \gamma_{\text{Bath}} + \gamma_{\text{SSET}} \quad (1a)$$

$$\gamma_{\text{NR}} T_{\text{NR}} = \gamma_{\text{Bath}} T_{\text{Bath}} + \gamma_{\text{SSET}} T_{\text{SSET}} \quad (1b)$$

As long as  $\gamma_{\text{NR}}$  is positive, equations (1a, 1b) provide a simple interpretation of the data in Fig. 2: as the coupling to the SSET is increased, the damping  $\gamma_{\text{SSET}}$  increases, so the effective temperature of the resonator is pulled away from  $T_{\text{Bath}}$  and closer to  $T_{\text{SSET}}$ . Experimentally,  $T_{\text{SSET}}$  is easily determined from the value of  $T_{\text{Bath}}$  where all the curves cross, or the value of  $T_{\text{NR}}$  when  $T_{\text{Bath}} \rightarrow 0$ : we find  $T_{\text{SSET}} \approx 200$  mK. The curvature observed in  $T_{\text{NR}}$  at high couplings is probably due to the temperature dependence of  $\gamma_{\text{Bath}}$ . Note that  $T_{\text{SSET}}$  is not determined by the thermodynamic temperature of the carriers in the SSET, but is a measure of the intensity of the charge fluctuations on the SSET.

Using the quantum noise approach<sup>3,16</sup>, we find that the back-action effects are determined by the asymmetric-in-frequency quantum noise spectrum of the back-action force,  $S_F(\omega)$ :

$$2m\hbar\omega_{\text{NR}}\gamma_{\text{SSET}} = S_F(\omega_{\text{NR}}) - S_F(-\omega_{\text{NR}}) \quad (2a)$$

$$4mk_{\text{B}}T_{\text{SSET}}\gamma_{\text{SSET}} = S_F(\omega_{\text{NR}}) + S_F(-\omega_{\text{NR}}) \quad (2b)$$

where  $k_{\text{B}}$  is Boltzmann's constant and  $m$  is the oscillator mass, and the positive (negative) frequency noise power describes the noise responsible for the rates of energy emission (absorption) from the nanoresonator to the SSET. Thus our nanomechanical resonator provides a frequency-resolved measurement of the asymmetric,

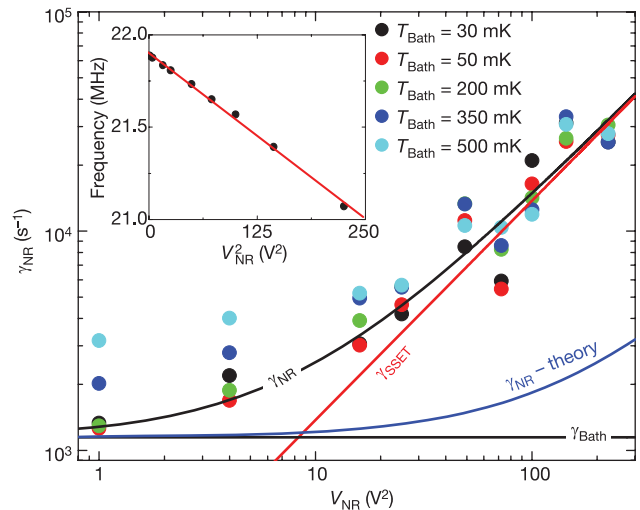
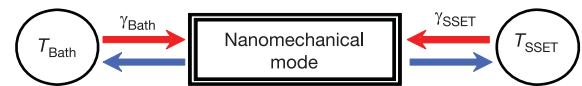


**Figure 3 | Resonator damping rate and frequency shift versus coupling voltage.** Main plot shows the measured nanoresonator dissipation rate,  $\gamma_{\text{NR}}$ , versus  $V_{\text{NR}}$  for various values of  $T_{\text{Bath}}$ . Inset shows the resonant frequency and damping rate to the SSET,  $\gamma_{\text{SSET}}$ , scale as  $V_{\text{NR}}^2$ , as expected (solid red lines). At low  $V_{\text{NR}}$ ,  $\gamma_{\text{NR}}$  is asymptotic to the damping rate to the bath,  $\gamma_{\text{Bath}}$  (black line). At high  $V_{\text{NR}}$ ,  $\gamma_{\text{NR}}$  is asymptotic to a quadratic dependence,  $\gamma_{\text{SSET}}$ , although at a rate 14 times higher than expected ( $\gamma_{\text{NR}}\text{-theory}$ , blue curve). Black curve shows  $\gamma_{\text{NR}} = \gamma_{\text{Bath}} + \gamma_{\text{SSET}}$ . The figure above shows the nanomechanical mode coupled to the thermal baths,  $T_{\text{Bath}}$  and  $T_{\text{SSET}}$ , through dissipative links,  $\gamma_{\text{Bath}}$  and  $\gamma_{\text{SSET}}$ . The red (blue) arrows indicate the emission (absorption) of quanta by the baths leading to heating (cooling) of the resonator.

quantum noise properties of the SSET<sup>17–19</sup>, albeit only at the resonator frequency.

When biased at a JQP, the transport is resonant and involves a process of Josephson and quasi-particle tunnelling. This leads to a simple expression for  $T_{\text{SSET}}$ :

$$k_{\text{B}}T_{\text{SSET}} = \frac{\hbar \Gamma^2 + 4(\Delta E/\hbar)^2}{4 \cdot 4\Delta E/\hbar} \quad (3)$$

where  $\Delta E$  is the difference between final and initial energies of the tunnelling Cooper pair, and  $\Gamma$  is the quasiparticle tunnel rate, which is essentially temperature independent far below the superconducting transition temperature. This result is analogous to laser ponderomotive cooling of a mechanical cavity<sup>20</sup>, or to Doppler cooling of a two-level atom<sup>21</sup>; hence we call this ‘Cooper-pair molasses’.

Figure 4 shows the sensitive dependence of  $T_{\text{NR}}$ ,  $\gamma_{\text{NR}}$  and  $\omega_{\text{NR}}$ , as we tune the SSET bias point through the two neighbouring JQP resonances. Between the two JQP peaks where  $\Delta E > 0$  (‘red detuned’),  $T_{\text{NR}}$  is in excellent agreement with the theoretical predictions ( $\sim 220$  mK) (Fig. 4d). The changes in frequency (Fig. 4b) are also reasonably well described, indicating that the overall magnitude of the non-fluctuating component of the back-action force is close to expectation. Only qualitative agreement is achieved for the damping, which results from a very small asymmetry in the force noise power (equation (2a)). We observe the expected quadratic dependence on

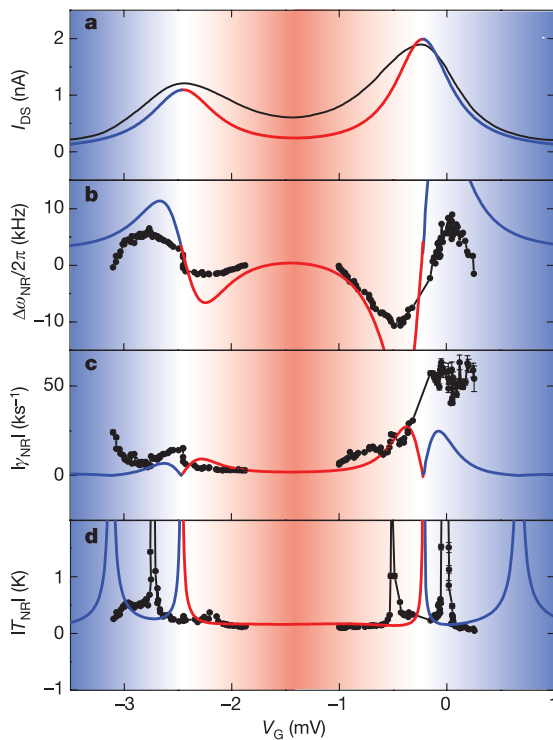


**Figure 4 | Back-action effects versus SSET bias point.** Comparison of experimental measurements (black points and lines) and theoretical predictions (blue and red lines) as  $V_{\text{G}}$  is scanned through neighbouring JQP resonances, with fixed  $V_{\text{DS}} = 4E_{\text{C}} - 100 \mu\text{V}$ , and  $V_{\text{NR}} = 5$  V, where  $E_{\text{C}}$  is the Coulomb energy of the SSET. The panels show **a**, the SSET current, **b**, the resonator frequency shift, **c**, the resonator damping rate,  $\gamma_{\text{NR}}$ , and **d**, the effective resonator temperature,  $T_{\text{NR}}$ . Note that in **c** the theoretically calculated values have been multiplied by a factor of 14. In **c** and **d**, expected unstable bias points,  $\{T_{\text{NR}}, \gamma_{\text{NR}}\} < 0$ , are shown in blue where SSET is ‘blue detuned’, and stable bias points,  $\{T_{\text{NR}}, \gamma_{\text{NR}}\} > 0$ , are shown in red where SSET is ‘red detuned’. Error bars are the standard deviation of the fitting parameters to the measured noise spectra.

$V_{\text{NR}}$  (Fig. 3) and the increase in damping as one approaches the JQP resonance (Fig. 4c). However, the magnitude is 14 times larger than expected. We believe that this excess may be related to the long-standing discrepancy between theory and experiment in transport characteristics at the JQP<sup>22</sup>. We do not believe that the excess damping observed is due to another independent bath, as the dissipation is clearly very sensitively controlled by the SSET bias point (Fig. 4).

Outside the JQP resonances, the tunnelling Cooper pairs can emit energy to the resonator ( $\Delta E < 0$ , ‘blue-detuned’), and the linear theory predicts negative SSET temperatures and damping rates<sup>10,11</sup>. When the predicted  $\gamma_{\text{NR}}$  becomes negative (region shaded blue in Fig. 4), states of small amplitude of motion are unstable with respect to a state of large amplitude motion of the resonator, where the amplitude is ultimately limited by nonlinearity in the dynamics<sup>10</sup>, and the picture of the SSET as an effective thermal bath breaks down. A theoretical description of our system in these parameter regions is beyond the scope of this Letter, but we do find experimentally points of dramatically increased  $T_{\text{NR}}$  outside the JQP peaks, as one would expect qualitatively. Additionally, we have observed the unstable behaviour when biasing the SSET at the double JQP, where the back-action effects are predicted to be larger than at the JQP<sup>10,11</sup>. Although we are only able to make quantitative comparison for the regions of stable bias, the fact that SSET operating points with opposite sign  $\Delta E$  yield the same current, but show very different back-action, provides compelling evidence that the SSET is the controlling source of the back-action fluctuations.

We can use equation (2) to calculate the amplitude of the back-action impulses and compare this to the uncertainty principle requirement,  $(S_x S_F)^{1/2} \geq \hbar/2$ , where  $S_x$  is the spectral power density of position (at our highest coupling voltage, we achieve  $\sqrt{S_x} = 3 \times 10^{-16} \text{ m Hz}^{-1/2}$ ). Using  $S_x = S_I/(dI/dx)^2$ , and  $S_I = 2eI$  at the JQP resonance<sup>23</sup>, we find  $\sqrt{S_F S_x} = 15\hbar/2$ , a factor of 15 larger than the uncertainty principle requirement. This excess back-action will limit the position resolution  $\Delta x$  to a factor of 3.9 over the quantum limit (Supplementary Information). However, this level of ideality is already sufficient for an SSET to enable the realization of novel quantum states of the mechanical resonator, including squeezed<sup>24</sup> and entangled states<sup>25</sup>.

The nanomechanical cooling and heating effects reported here are closely related to proposed processes using a Cooper-pair qubit<sup>26,27</sup> and a quantum dot<sup>28,29</sup>, and are (to our knowledge) the first examples of the interaction between coherent electronics and nanomechanical modes. Although the cooling power of our Cooper-pair molasses is exceedingly small,  $\dot{Q} \approx \gamma_{\text{SSET}} k_{\text{B}}(T_{\text{Bath}} - T_{\text{SSET}}) = 10^{-21}$  W, it is sufficient to cool a single, well isolated, mechanical degree of freedom. Furthermore, we believe that it is possible to use this method to produce ultracold, quantum states in nanomechanical systems with high resistance tunnel junctions, as it is expected<sup>10</sup> that  $T_{\text{SSET}} \propto R_{\text{J}}^{-1}$  and  $\gamma_{\text{SSET}} \propto R_{\text{J}}^2$ , providing increasing coupling to a decreasing temperature bath as the junction resistance,  $R_{\text{J}}$ , is increased. For instance, the junctions reported in ref. 30 should reach a minimum  $T_{\text{SSET}} = 0.3$  mK, providing access to the quantum ground state of a resonator similar to that reported here.

Received 17 February; accepted 30 June 2006.

1. Caves, C. M. Quantum limits on noise in linear amplifiers. *Phys. Rev. D* **26**, 1817–1839 (1982).
2. Braginsky, V. B. & Khalili, F. Ya. *Quantum Measurement* (Cambridge Univ. Press, Cambridge, 1995).
3. Clerk, A. A. Quantum-limited position detection and amplification: A linear response perspective. *Phys. Rev. B* **70**, 245306 (2004).
4. Abbott, B. et al. Upper limits on gravitational wave bursts in LIGO’s second science run. *Phys. Rev. D* **72**, 062001 (2005).
5. Rugar, D., Budakian, R., Mamin, H. J. & Chui, B. W. Single spin detection by magnetic resonance force microscopy. *Nature* **430**, 329–332 (2004).
6. Tittonen, I. et al. Interferometric measurements of the position of a macroscopic body: Towards observations of quantum limits. *Phys. Rev. A* **59**, 1038–1044 (1999).

7. LaHaye, M. D., Buu, O., Camarota, B. & Schwab, K. C. Approaching the quantum limit of a nanomechanical resonator. *Science* **304**, 74–77 (2004).
8. Schoelkopf, R. J., Wahlgren, P., Kozhevnikov, A. A., Delsing, P. & Prober, D. The radio-frequency single-electron transistor (RF-SET): A fast and ultrasensitive electrometer. *Science* **280**, 1238–1242 (1998).
9. Fulton, T. A., Gammel, P. L., Bishop, D. J., Dunkleberger, L. N. & Dolan, G. J. Observation of combined Josephson and charging effects in small tunnel junction circuits. *Phys. Rev. Lett.* **63**, 1307–1310 (1989).
10. Clerk, A. A. & Bennett, S. Quantum nano-electromechanics with electrons, quasiparticles and Cooper pairs: effective bath descriptions and strong feedback effects. *N. J. Phys.* **7**, 238 (2005).
11. Blencowe, M. P., Imbers, J. & Armour, A. D. Dynamics of a nanomechanical resonator coupled to a superconducting single-electron transistor. *N. J. Phys.* **7**, 236 (2005).
12. Mozyrsky, D., Martin, I. & Hastings, M. B. Quantum-limited sensitivity of single-electron-transistor-based displacement detectors. *Phys. Rev. Lett.* **92**, 018303 (2004).
13. Armour, A. D., Blencowe, M. P. & Zhang, Y. Classical dynamics of a nanomechanical resonator coupled to a single-electron transistor. *Phys. Rev. B* **69**, 125313 (2004).
14. Mozyrsky, D. & Martin, I. Quantum-classical transition induced by electrical measurement. *Phys. Rev. Lett.* **89**, 018301 (2002).
15. Ojha, R. P., Lemieux, P.-A., Dixon, P. K., Liu, A. J. & Durian, D. J. Statistical mechanics of a gas-fluidized particle. *Nature* **427**, 521–523 (2004).
16. Clerk, A. A., Girvin, S. M., Nguyen, A. K. & Stone, A. D. Resonant Cooper-pair tunneling: quantum noise and measurement characteristics. *Phys. Rev. Lett.* **89**, 176804 (2002).
17. Gavish, U., Levinson, Y. & Imry, Y. Detection of quantum noise. *Phys. Rev. B* **62**, R10637 (2000).
18. Schoelkopf, R. J., Clerk, A. A., Girvin, S. M., Lehnert, K. W. & Devoret, M. H. in *Quantum Noise in Mesoscopic Physics* (Kluwer Academic, Norwell, Massachusetts, 2003).
19. Deblock, R., Onac, E., Gurevich, L. & Kouwenhoven, L. P. Detection of quantum noise from an electrically driven two-level system. *Science* **301**, 203–206 (2003).
20. Braginsky, V. B. & Vyatchanin, S. P. Low quantum noise tranquilizer for Fabry-Perot interferometer. *Phys. Lett. A* **293**, 228–234 (2002).
21. Lett, P. D. *et al.* Optical molasses. *J. Opt. Soc. Am. B* **6**, 2084–2107 (1989).
22. Pohlen, S. L., Fitzgerald, R. J. & Tinkham, M. The Josephson-quasiparticle (JQP) current cycle in the superconducting single-electron transistor. *Physica B* **284–288**, 1812–1813 (2000).
23. Choi, M.-S., Plastina, F. & Fazio, R. Charge and current fluctuations in a superconducting single-electron transistor near a Cooper pair resonance. *Phys. Rev. B* **67**, 045105 (2003).
24. Ruskov, R., Schwab, K. & Korotkov, A. N. Squeezing of a nanomechanical resonator by quantum nondemolition measurement and feedback. *Phys. Rev. B* **71**, 235407 (2005).
25. Armour, A. D., Blencowe, M. P. & Schwab, K. C. Entanglement and decoherence of a micromechanical resonator via coupling to a Cooper-pair box. *Phys. Rev. Lett.* **88**, 148301 (2002).
26. Irish, E. K. & Schwab, K. Quantum measurement of a coupled nanomechanical resonator-Cooper-pair box system. *Phys. Rev. B* **68**, 155311 (2003).
27. Martin, I., Shnirman, A., Tian, L. & Zoller, P. Ground-state cooling of mechanical resonators. *Phys. Rev. B* **69**, 125339 (2004).
28. Wilson-Rae, I., Zoller, P. & Imamoglu, A. Laser cooling of a nanomechanical resonator mode to its quantum ground state. *Phys. Rev. Lett.* **92**, 075507 (2004).
29. Lundin, U. Localized heating or cooling in mesoscopic devices by electron transport. *Phys. Lett. A* **332**, 127–130 (2004).
30. Nakamura, Y., Pashkin, Yu. A. & Tsai, J. S. Coherent control of macroscopic quantum states in a single-Cooper-pair box. *Nature* **398**, 786–788 (1999).

**Supplementary Information** is linked to the online version of the paper at [www.nature.com/nature](http://www.nature.com/nature).

**Acknowledgements** We thank A. Rimberg and A. Vandaley for discussions, and B. Camarota for assistance with the fabrication of the samples. M.P.B. is supported by the NSF through an NIRT grant, A.D.A. is supported by the EPSRC, and A.A.C. is supported by NSERC.

**Author Contributions** A.N. and O.B. contributed equally to this work.

**Author Information** Reprints and permissions information is available at [www.nature.com/reprints](http://www.nature.com/reprints). The authors declare no competing financial interests. Correspondence and requests for materials should be addressed to K.C.S. ([schwab@ccmr.cornell.edu](mailto:schwab@ccmr.cornell.edu)).